Research Article

Anion Effect of Zinc Source on Chemically Deposited ZnS(O,OH) Films

K. Ernits, K. Muska, M. Danilson, J. Raudoja, T. Varema, O. Volobujeva, and M. Altosaar

Department of Material Science, Tallinn University of Technology, Ehitajate tee 5, Tallinn 19086, Estonia

Correspondence should be addressed to K. Ernits, whiisu@msn.com

The study on the anion effect of different Zn sources—$Zn(CH_3COO)_2$, $ZnCl_2$, ZnI_2, $Zn(NO_3)_2$ and $ZnSO_4$—on the chemical deposition of ZnS(O,OH) films revealed that the growth rate and composition of the ZnS(O,OH) layer depend on the instability constant (pK) value of the corresponding Zn-complex $Zn(L)_n$ in the chemical bath solution. In the region of $pK_{Zn(NH3)2+} > pK_{Zn(L)n}$ the ZnS(O,OH) film's growth rate and ZnS concentration in films increased with the increasing pK value of the used Zn salt complex up to the pK value of the $Zn[NH_3]^{2+}$ complex and decreased in the region where $pK_{Zn(NH3)2+} < pK_{Zn(L)n}$. The band gap values (around 3.6 eV in most cases) of deposited ZnS(O,OH) films did not depend on the Zn precursor's instability constant, the ZnS(O,OH) film from zinc nitrate containing bath has higher band gap energy (E_g = 3.8 eV). The maximum efficiency of CISSe and CZTSSe monograin layer solar cells was gained with ZnS(O,OH) buffer layer deposited from CBD solution containing $Zn(CH_3COO)_2$ as Zn source, which provided the highest growth rate and ZnS concentration in the ZnS(O,OH) film on glass substrates.

1. Introduction

ZnS is beside CdS the second most investigated buffer layer material for $CuInSe_2$ (CISe) type solar cells. ZnS is an attractive material mainly because of its wide band gap of 3.7 eV [1], which makes it more transparent in the short wavelength region between 350 and 550 nm compared to CdS with the band gap value of 2.4 eV [1]. A chemical bath deposition (CBD) is the most commonly used process for ZnS buffer formation on the top of a CISe type absorber. So far, the highest demonstrated CBD-ZnS/Cu(In,Ga)Se$_2$ (CIGSe) solar cell efficiency is 18.6% as reported by NREL [2], while the highest efficiency obtained with CdS is 19.9% [3]. The high-efficiency ZnS/CIGSe solar cells were prepared also by the Nakada process [4], where zinc sulphate was used as the zinc source, thiourea as the sulphur source and ammonia as the complexing agent.

The present work aimed to study the impact of Zn precursor anion on the CBD-ZnS film's growth rate and properties. There are only few papers in the literature where the influence of different anion types in the ZnS deposition solution on thin film parameters was studied [5–7]. Eshuis et al. [5] pointed out that the chemical nature of used anions controls the growth rate, and morphology of ZnS particles. Several authors have studied CdS films deposited from different cadmium salts in ammonia solutions [8–10] and ZnO deposition from different zinc sources [11] as well. A change in the electrical resistivity, growth rate and particle size of the films with changes in chemical nature of anions in chemical bath solution was detected, but those changes did not lead to the changes in efficiencies of CISe solar cells [9]. Khallaf et al. [8] found that higher values of instability constants of the different cadmium complexes in the deposition solution led to the thinner CdS films. As the deposited CBD-ZnS films contain in addition to ZnS also $Zn(OH)_2$ and ZnO, it is typical to mark them as ZnS(O,OH). In this study CBD-ZnS films were deposited from different Zn sources. The growth rate of the films along with compositional and optical properties presented together with photovoltaic characteristics of $CuIn(S,Se)_2$ (CISSe), and $Cu_2ZnSn(S,Se)_4$ (CZTSSe) monograin layer (MGL) solar cells with CBD ZnS(O,OH) buffer layers.

2. Experimental Details

2.1. ZnS(O,OH) Film Deposition and Characterization. ZnS(O,OH) thin films were deposited on soda lime glass (SLG) substrates. Freshly prepared water solutions contained 0.32 M $SC(NH_2)_2$ (thiourea (TU), 7.5 M ammonia and 0.16 M Zn precursor salt: $Zn(CH_3COO)_2 \cdot 2H_2O$ ($Zn(Ac)_2$), $ZnCl_2, ZnI_2, Zn(NO_3)_2 \cdot 4H_2O, ZnSO_4 \cdot 7H_2O$. SLG substrates were cleaned with concentrated H_2SO_4 and rinsed with deionized (DI, $18 M\Omega \cdot cm$) water. All the used chemicals were pro analysi grade from Merck. The CBD solutions were prepared by dissolution of the Zn salt and TU in DI water separately and the two solutions were mixed at $85°C$ by continuous stirring. After 5 minutes the NH_3 solution was added and substrates were dipped into the bath solution. The deposition process was stopped after 30 minutes by lifting the substrates out of the CBD solution. The deposited films were annealed in a semi closed quartz tube in conditions of continuous vacuum pumping at $220°C$ for 10 minutes.

Scanning Electron Microscopy (HR-SEM Zeiss ULTRA 55) was used to measure the thickness of the films. X-ray Photoelectron Spectroscopy (Kratos Axis Ultra DLD, monochromatic Al Kα radiation) was used to determine the Zn:S:O concentrations ratio in the films. Spectrophotometer with an integrating sphere (Jasco V-670 UV-VIS-NIR) was used to measure the optical transmission and to determine the optical band gaps of the ZnS(O,OH) films.

2.2. $CuIn(Se,S)_2$ and $Cu_2ZnSn(S,Se)_4$ Solar Cell Preparation and Characterization. Monograin layer (MGL) CISSe and CZTSSe solar cells were prepared as published elsewhere [12, 13]. CBDs ZnS(O,OH) films were deposited on the CISSe and CZTSSe monograin membranes at the solution temperature of $85°C$ for 5 minutes.
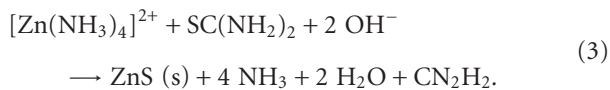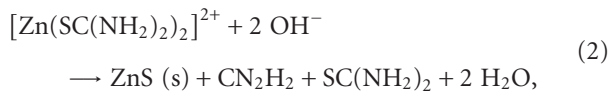
Prepared solar cells were characterized by current-voltage measurements, which were carried out in the darkness and under illumination of $100 \, mW \, cm^{-2}$.

3. Results and Discussion

3.1. Chemical Route to ZnS(O,OH) Deposition and the Anion Effect. In the chemical bath solution, Zn-salt molecules decompose to ions and Zn^{2+} can form different complexes as follows:

$$2Zn^{2+} + 2 SC(NH_2)_2 + 4NH_3$$
$$\longrightarrow [Zn(SC(NH_2)_2)_2]^{2+} + [Zn(NH_3)_4]^{2+}. \tag{1}$$
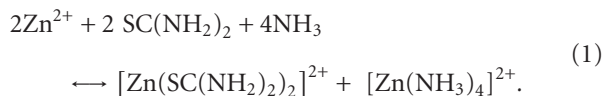
We assume that the formation of solid (s) ZnS(O,OH) results through the decomposition of the following complexes in aqua deposition solutions by (2) and (3) as

$$[Zn(SC(NH_2)_2)_2]^{2+} + 2 OH^-$$
$$\longrightarrow ZnS (s) + CN_2H_2 + SC(NH_2)_2 + 2 H_2O, \tag{2}$$

$$[Zn(NH_3)_4]^{2+} + SC(NH_2)_2 + 2 OH^-$$
$$\longrightarrow ZnS (s) + 4 NH_3 + 2 H_2O + CN_2H_2. \tag{3}$$

Simultaneously to ZnS formation, zinc hydroxide can form in the ammonia containing solution as follows:

$$Zn^{2+} + 2 OH^- \longrightarrow Zn(OH)_2(s). \tag{4}$$
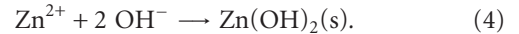
The deposited films were annealed in vacuum at $220°C$ for 10 minutes to dehydrate $Zn(OH)_2$ (5):

$$Zn(OH)_2 \longrightarrow ZnO (s) + H_2O \quad (T = 125°C). \tag{5}$$
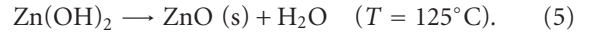
(see [14]). The anions from the used zinc salts play a role in the growth of ZnS(O,OH) films as additional complexing agents, forming $Zn(Ligand)_n(Zn(L)_n)$ complexes besides $[Zn(NH_3)_4]^{2+}$ and $[Zn(OH)_4]^{2+}$ in the chemical bath solution. $Zn(L)_n$ complexes have different instability constants according to the anions (see Table 1). The instability constants were calculated for poorly dissociating complexes only; therefore, the instability constant for $Zn(NO_3)_2$ is not given.

Square brackets in Table 1 imply the concentrations. A high value of the instability constant pK_1 shows that the complex ion is easily formed, therefore the $Zn(L)_1$ complex with OH^- ion is the most stable complex in the series.

3.2. The Results of ZnS(O,OH) Films Measurements.

3.2.1. The Cluster Size and Thickness of ZnS(O,OH) Films. SEM micrographs (presented elsewhere [16]) revealed that change in zinc sources affects the size of ZnS(O,OH) clusters and the film thickness grown on SLG. The ZnS(O,OH) film thickness depending on the instability constant pK_n values of corresponding complex ions is presented in Figure 1. The thickest films with the largest clusters grew from $Zn(Ac)_2$ containing chemical solution. ZnS(O,OH) films with the smallest clusters grew from $ZnCl_2$ and $Zn(NO_3)_2$ containing solutions. ZnS(O,OH) film thickness increases with the instability constant values in the region (a) where $pK_{Zn(NH3)2+} > pK_{Zn(L)n}$ and decreases after the $Zn[NH_3]^{2+}$ complex line.

3.2.2. The Composition of ZnS(O,OH) Films. XPS compositional measurements revealed that the ZnS(O,OH) films contain $Zn(OH)_2$ and ZnO besides ZnS. The concentration of ZnS in the ZnS(O,OH) films is given in Figure 2 (black stars). The obtained results show that the content of ZnS in ZnS(O,OH) film is dependent on the instability constant of the zinc precursor complex. The content of ZnS in the films increases with the value of instability constants of $Zn[L]_n$ complex in the region (a) and drops after the $Zn[NH_3]^{2+}$ complex line in region (b). This is the indication of low deposition rate of ZnS and high deposition rate of $Zn(O,OH)_2$ in the region (b) where $Zn[L]_n$ complex is stronger than $Zn[NH_3]^{2+}$ complex.

XPS measurements revealed detectable amounts (below 1 mole %) of several impurities in ZnS(O,OH) films from $Zn(NO_3)_2$ (Cl), ZnI_2 (Cd, Cl, N), and $Zn(Ac)_2$ (N).

XPS measurements showed also that the annealing process in vacuum at $200°C$ for 10 minutes was not sufficient to dehydrate $Zn(OH)_2$ completely. It was the most successful

TABLE 1: Instability constants pK of Zn complexes [15].

| Decomplexation reactions of Zn(L)$_1$	Calculation of equilibrium constant (K_1) for the reaction	Instability constant of Zn complex ion $pK_1 = -\log K_1$ (at 25°C)
Zn(OH)$^+$ $\longleftrightarrow$ Zn^{2+} + OH	[Zn^{2+}] · [OH$^-$]/[Zn(OH)$^+$]	4.4
Zn(NH$_3$)$^{2+}$ $\longleftrightarrow$ Zn^{2+} + NH$_3$	[Zn^{2+}] · [NH$_3$]/[Zn(NH$_3$)$^{2+}$]	2.2
Zn(TU)$^{2+}$ $\longleftrightarrow$ Zn^{2+} + TU	[Zn^{2+}] · [TU]/[Zn(TU)$^{2+}$]	0.5
Zn(SO$_4$)^0 $\longleftrightarrow$ Zn^{2+} + SO$_4^{2-}$	[Zn^{2+}] · [SO$_4^{2-}$]/[Zn(SO$_4$)^0]	2.3
Zn(Ac)$^+$ $\longleftrightarrow$ Zn^{2+} + Ac$^-$	[Zn^{2+}] · [Ac$^-$]/[Zn (Ac)$^+$]	1.6
Zn(Cl)$^+$ $\longleftrightarrow$ Zn^{2+} + CI$^-$	[Zn^{2+}] · [Cl$^-$]/[Zn(Cl)$^-$]	−0.5
Zn(I)$^+$ $\longleftrightarrow$ Zn^{2+} + I$^-$	[Zn^{2+}] · [I$^-$]/[Zn(l)$^-$]	−2.9
Zn(NO$_3$)$_2$ $\longleftrightarrow$ Zn^{2+} + 2NO$_3^-$		Unstable compound
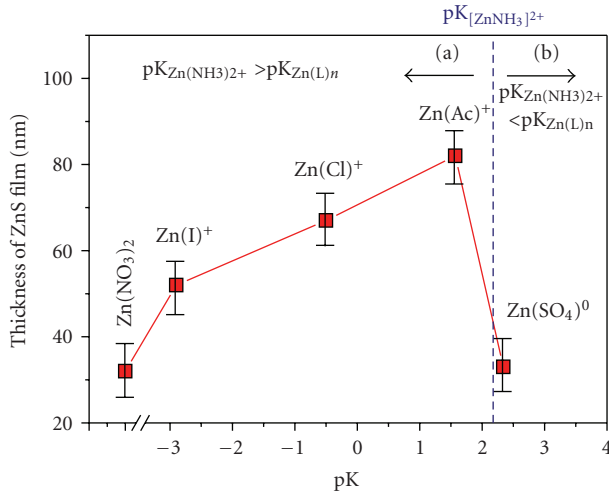
FIGURE 1: Thickness of ZnS(O,OH) films deposited from 5 different Zn sources versus pK (instability constant). The blue dashed line indicates Zn[NH$_3$]$^{2+}$ complex line, which divides the graph into two regions where (a) pK$_{Zn(NH3)2+}$ > pK$_{Zn(L)n}$ and (b) pK$_{Zn(NH3)2+}$ < pK$_{Zn(L)n}$.
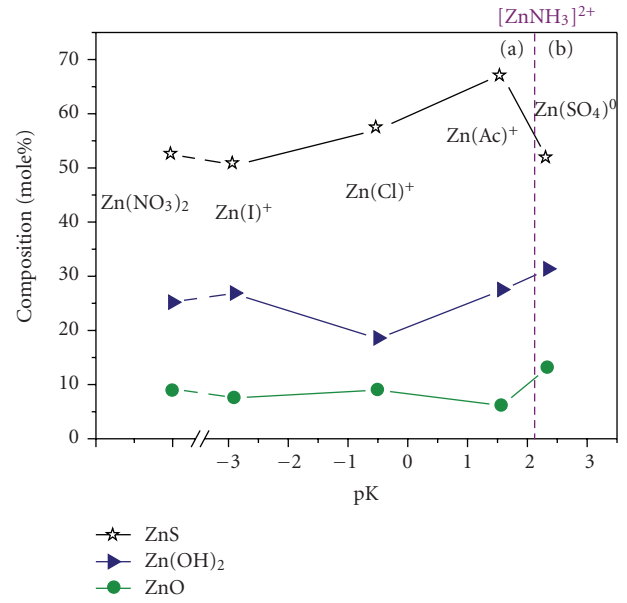

FIGURE 2: The composition of ZnS(O,OH) films versus pK (instability constant) of Zn complexes. The films contain mainly ZnS (stars), ZnO (circles), and Zn(OH)$_2$ (triangles).

for the ZnS(O,OH) film with smallest clusters, deposited from chemical bath containing ZnCl$_2$.

3.2.3. The Optical Transmission and Band Gaps of ZnS(O,OH) Films. The results of optical transmission measurements are brought in Figure 3 (squares). In region (a) films transmission decreases with increasing instability constant values and increases after the Zn[NH$_3$]$^{2+}$ complex line in region (b) where pK$_{Zn(L)n}$ > pK$_{Zn(NH3)2+}$, probably due to the variations in film thickness.

The optical absorption coefficient (α) was deduced from the transmission and reflectance spectra, using the relation $\alpha = -\ln(T_{cor})$, where as T_{cor} was calculated $T_{cor} = T \cdot (1 - R)$ from the intensities of the transmitted (T) and reflected (R) lights. A plot of the value of $(\alpha h\nu)^2$ against photon energy ($h\nu$) shows a straight line portion, and the intercept of this linear portion on the energy axis at $(\alpha h\nu)^2$ equal to zero gives the band gap of the material. The values of optical band gap energy in Figure 3 are in the range of 3.6 eV, except 3.8 eV for the ZnS deposited from Zn(NO$_3$)$_2$. Similar results are

described in [6] where higher band gap values (3.75–3.93 eV) were gained for CBD-ZnS films deposited from Zn(NO$_3$)$_2$ in comparison with those ones from ZnCl$_2$ (3.66–3.78 eV) [6]. The results could be explained with different crystal structure of the ZnS films from Zn(NO$_3$)$_2$ and ZnCl$_2$, since hexagonal ZnS has larger band gap for (3.67 eV [1], 3.74 eV [17],) than that of cubic ZnS (3.54 eV [1] and 3.66 eV [17]).

3.3. The Results of CuIn(SSe)$_2$ and Cu$_2$(ZnSn)(SSe)$_4$ Solar Cells Measurements

3.3.1. Current-Voltage Characteristics of MGL Solar Cells. The values of open circuit voltages and fill factors were only very slightly affected by the variation of ZnS(O,OH) deposition precursor. Current densities of CBD-ZnS/Cu(In)Se$_2$ mono-grain layer solar cells changed with instability constants of Zn-ligand complexes following the same law as that of the growth rate of ZnS(O,OH) films (Figure 4). Figure 4 shows
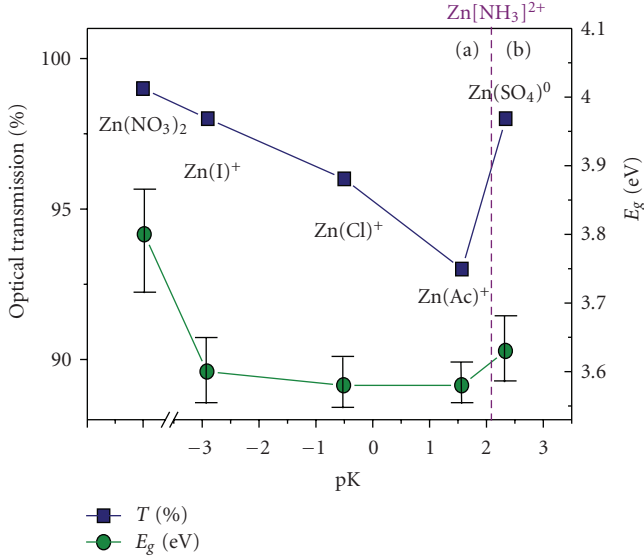
FIGURE 3: Optical transmission (blue squares) and band gap values (green circles) of ZnS(O,OH) films versus instability constant of Zn complex. The dashed line indicates $Zn[NH_3]^{2+}$ complex line.
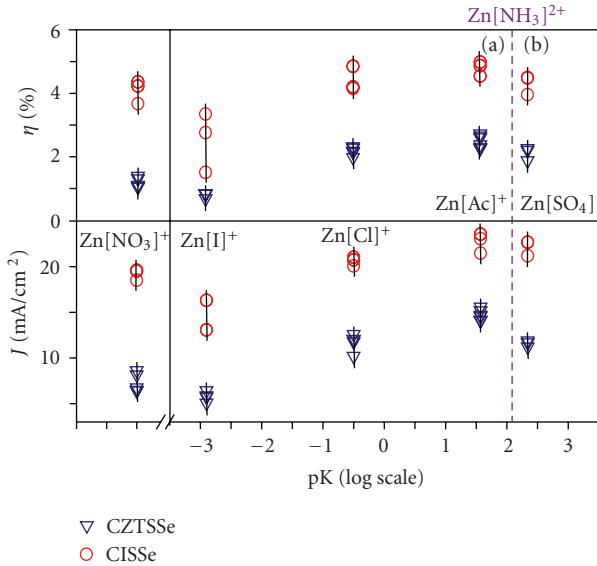

FIGURE 4: Current densities and efficiencies of CISSe (red) and CZTSSe (blue) MGL solar cells versus Zn-complex instability constant values from various zinc precursors. The dashed line indicates $Zn[NH_3]^{2+}$ complex line, which divides the graph to two regions: (a) $pK_{Zn(NH3)2+} > pK_{Zn(L)n}$ and (b) $pK_{Zn(L)n} > pK_{Zn(NH3)2+}$.

that the CISSe and CZTSSe solar cells with ZnS(O,OH) films from ZnI2 with relatively high resistivity and high impurity content in the films have the lowest current densities. The solar cell efficiency curves follow the shape of current density curves (Figure 4). The dependence can be caused by the different thickness of ZnS(O,OH) films and the content of ZnS and impurities in the films. The only exceptions are solar cells with ZnS(O,OH) from $Zn(NO_3)_2$, which have the highest transmission and the largest band gap.

3.4. Discussions. The idea that anions from different zinc salts as Zn sources in the chemical solution for ZnS(O,OH) deposition can act as complexing agents and influence the deposition process was supported by experimental findings. The comparison of values of instability constants (see Table 1) shows that $Zn(SO_4)^0$ complex is stronger than $Zn(NH_3)^{2+}$ complex and the other $Zn(L)_1$ complexes. This fact probably affects ZnS(O,OH) films growth in the way that the stronger $Zn(SO_4)^0$ complex drives (1) left (see Section 3.1), which results in lower ZnS deposition rates and smaller thicknesses. Lower deposition rates increase the time for the deposition process and can result in thinner films with poor coverage on the top of the absorber in solar cells. Poor coverage of the buffer layer can induce shunts in solar cells. From the solar cell results we can see that solar cells with thickest ZnS(O,OH) have highest current densities.

On the other hand, $Zn(OH)_4^{2+}$ complex is stronger than $Zn(NH_3)^{2+}$ complex and drives (4) right (see Section 3.1), resulting in $Zn(OH)_2$ rich films from $ZnSO_4$ containing chemical bath solution. The variations of ZnS, ZnO and $Zn(OH)_2$ content in CBD-ZnS change the material optical properties like transmission and also the value of band gap energy. The usage of ZnS with about 1 eV higher band gap energy (3.6 eV) as buffer material in solar cells instead of usually used CdS (E_g = 2.4 eV) can result in two effects in solar cell as follows.

(1) More light passes the buffer layer, increasing the light absorption in absorber layer, which increases the current densities of solar cells in the case of ZnS.

(2) There might occur the so-called "spike" in solar cell *p-n* junction reducing current collection of the solar cell with ZnS buffer layer [18].

Additionally, ZnO with band gap energy around 3.2 eV in the buffer material can reduce both effects, opposite to $Zn(OH)_2$ with higher band gap energy value than ZnS. $Zn(OH)_2$ has generally lower transmission and it can reduce CBD-ZnS transmission, if not dehydrated from the film; therefore, ZnO is preferable over $Zn(OH)_2$ as a coproduct in CBD-ZnS film. But the lattice constants of ZnS (*a* = 3.8 hexagonal and 5.4 cubic Å) match better with currently used absorber material (*a* = 5.4–5.8 Å) than ZnO (*a* = 3.2 Å); therefore, CBD-ZnS should contain mainly ZnS [19]. As a result, we can find that solar cells with ZnS(O,OH) buffer layer deposited from Zn(Ac)2, where the highest concentration of ZnS was found, had highest solar cell current densities and efficiencies.

4. Conclusions

The study on the anion effect of the Zn source for the chemical deposition of ZnS(O,OH) films revealed that the growth rate and composition of ZnS(O,OH) layer depend on the instability constant value of Zn complex in chemical bath solution. The ZnS(O,OH) film's growth rate and ZnS concentration in films increased with the increasing value of Zn precursor's instability constant up to the $Zn[NH_3]^{2+}$ complex but decreased after that. The analogous effect of chemical nature of anion was detected for solar cell current

densities and efficiencies. The highest solar cell current densities and efficiencies were achieved with ZnS(O,OH) buffer layers with the highest growth rate and ZnS content, deposited from $Zn(Ac)_2$. The only exception was solar cell with ZnS(O,OH) deposited from $Zn(NO_3)_2$ containing bath, which results in ZnS(O,OH) with the widest band gap (3.8 eV) and the highest transmission.

Acknowledgments

References

[1] D. R. Lidle, *Handbook of Chemistry and Physics*, CRC Press, Boca Raton, Fla, USA, 78th edition, 1997-1998.

[2] D. Hariskos, S. Spiering, and M. Powalla, "Buffer layers in Cu(In,Ga)Se$_2$ solar cells and modules," *Thin Solid Films*, vol. 480-481, pp. 99–109, 2005.

[3] I. Repins, M. A. Contreras, B. Egaas, et al., "19.9%-efficient ZnO/CdS/CuInGaSe^2 solar cell with 81.2% fill factor," *Progress in Photovoltaics: Research and Applications*, vol. 16, no. 3, pp. 235–239, 2008.

[4] T. Nakada, M. Mizutani, Y. Hagiwara, and A. Kunioka, "High-efficiency Cu(In,Ga)Se$_2$ thin-film solar cells with a CBD-ZnS buffer layer," *Solar Energy Materials and Solar Cells*, vol. 67, no. 1–4, pp. 255–260, 2001.

[5] A. Eshuis, G. R. A. van Elderen, and C. A. J. Koning, "A descriptive model for the homogeneous precipitation of zinc sulfide from acidic zinc salt solutions," *Colloids and Surfaces A*, vol. 151, no. 3, pp. 505–512, 1999.

[6] A. Antony, K. V. Murali, R. Manoj, and M. K. Jayaraj, "The effect of the pH value on the growth and properties of chemical-bath-deposited ZnS thin films," *Materials Chemistry and Physics*, vol. 90, no. 1, pp. 106–110, 2005.

[7] Y. Zhao, J.-M. Hong, and J.-J. Zhu, "Microwave-assisted self-assembled ZnS nanoballs," *Journal of Crystal Growth*, vol. 270, no. 3-4, pp. 438–445, 2004.

[8] H. Khallaf, I. O. Oladeji, G. Chai, and L. Chow, "Characterization of CdS thin films grown by chemical bath deposition using four different cadmium sources," *Thin Solid Films*, vol. 516, no. 21, pp. 7306–7312, 2008.

[9] M. Altosaar, K. Ernits, J. Krustok, T. Varema, J. Raudoja, and E. Mellikov, "Comparison of CdS films deposited from chemical baths containing different doping impurities," *Thin Solid Films*, vol. 480-481, pp. 147–150, 2005.

[10] R. Ortega-Borges and D. Lincot, "Mechanism of chemical bath deposition of cadmium sulfide thin films in the ammonia-thiourea system," *Journal of the Electrochemical Society*, vol. 140, no. 12, pp. 3464–3473, 1993.

[11] E. Bacaksiz, M. Parlak, M. Tomakin, A. Özcelik, M. Karakiz, and M. Altunbas, "The effects of zinc nitrate, zinc acetate and zinc chloride precursors on investigation of structural and optical properties of ZnO thin films," *Journal of Alloys and Compounds*, vol. 466, no. 1-2, pp. 447–450, 2008.

[12] M. Altosaar, A. Jagomägi, M. Kauk, et al., "Monograin layer solar cells," *Thin Solid Films*, vol. 431-432, pp. 466–469, 2003.

[13] M. Altosaar, J. Raudoja, K. Timmo, et al., "Cu$_2$Zn$_{1-x}$Cd$_x$Sn(Se$_{1-y}$S$_y$)$_4$ solid solutions as absorber materials for solar cells," *Physica Status Solidi A*, vol. 205, no. 1, pp. 167–170, 2008.

[14] *Handbook of Chemistry II*, Izdatelstvo Himia, Moscow, Russia, 1965.

[15] J. J. Loure, *Handbook of Analythical Chemistry*, Izdatelstvo Himia, Moscow, Russia, 1965.

[16] K. Ernits, K. Muska, M. Kauk, et al., "Chemical bath deposition of ZnS films using different Zn-salts," in *Proceedings of the E-MRS Spring Meeting Symposium*, Strasbourg, France, June 2009, poster BP4-10.

[17] *Physics of A^{II}B^{VI} Compounds*, Nauka, Moscow, Russia, 1986.

[18] T. Minemoto, T. Matsui, H. Takakura, et al., "Theoretical analysis of the effect of conduction band offset of window/CIS layers on performance of CIS solar cells using device simulation," *Solar Energy Materials and Solar Cells*, vol. 67, no. 1–4, pp. 83–88, 2001.

[19] K. Ernits, *Study of In$_2$S$_3$ and ZnS thin films deposited by ultrasonic spray pyrolysis and chemical deposition*, dissertation, Tallinn University of Technology, Tallinn, Estonia, 2009.